

# CT value organ and homogeneous assigned methods-based radiation treatment planning of pelvic cavity tumors

D.Z. Jiang<sup>1</sup>, Z.T. Dai<sup>2</sup>, Z.R. Bao<sup>1</sup>, H. Liu<sup>1\*</sup>, H.L. Zhao<sup>1</sup>, C.H. Xie<sup>1</sup>,  
C. Chen<sup>1</sup>, Y.F. Zhou<sup>1</sup>, J. Zhang<sup>1\*</sup>

<sup>1</sup>Department of Radiation and Medical Oncology, Hubei Key Laboratory of Tumor Biological Behaviors, Hubei

<sup>2</sup>Cancer Clinical Study Center, Zhongnan Hospital of Wuhan University, Wuhan, China, 430071

School of Physics and Technology, Wuhan University, Wuhan, China, 430072

## ABSTRACT

**Objective:** By dividing the CT value into different intervals, the authors aimed to investigate the effect of CT value variation on dosimetric results and propose a method to combine MRI with assigned CT values. **Materials and Methods:** Imaging data were analyzed from thirty patients in three different regions by a treatment planning system. The average CT value of each tissue or organ, standard deviation and 95% confidence interval were obtained by the Eclipse treatment planning system. Fifteen patients were included in this study by IMRT. Eclipse was used for all delineations, registrations, and dose calculations. In the synthetic CT image, the CT values of the target and OAR were assigned according to the sampled CT value above. The homogeneous assigned method divides the human tissue CT image into another synthetic CT image that only assigns bones and water. Dosimetric differences and dose homogeneity were compared under the same dose and field conditions. **Results:** By dividing the CT value with the interval method and verifying it with dose calculation, different CT value intervals can reflect different human tissues or organs. The effect of CT value variation between -100 HU and 100 HU on dose calculation is within 2%. Compared with the same treatment plan on different CT images, there is little deviation between the synthetic CT image and the original CT image. The  $D_{max}$ ,  $D_{mean}$ ,  $D_{mean}$ ,  $D_{98\%}$ ,  $D_{95\%}$ ,  $D_{5\%}$ , and  $D_{2\%}$  of PTV are all below 1.61%, and the dose percentage and volume percentage of OAR are below 1.86%. **Conclusion:** The combination of MRI with assigned CT values is feasible for the performance of MR alone in pelvis tumor treatment plans.

**Keywords:** CT value interval, organ assigned, homogeneous assigned, cervical carcinoma, dose calculation, TPS.

## ► Original article

### \*Corresponding authors:

Dr. Zhang Jun, Dr. Hui Liu,

Fax: +86 176 7179 1257

E-mail: 47944157@qq.com

Revised: April 2018

Accepted: July 2018

Int. J. Radiat. Res., July 2019;

17(3): 667-674

DOI: 10.18869/acadpub.ijrr.17.3.667

## INTRODUCTION

Computed tomography (CT) numbers can provide accurate information regarding the density of human tissues. CT images are conventionally applied to external radiotherapy treatment planning (RTP) because of the possibility of calibrating CT image Hounsfield units (HUs) into electron density information. Accurate information on electron density, which is used for inhomogeneity corrections by

treatment planning systems (TPS), is considered crucial in radiation therapy dose calculations<sup>(1,2)</sup>.

CT has been the basis for treatment planning because of its availability, high geometrical accuracy, and direct connection to electron density used in dose calculations. However, it is clear that CT alone does not always provide sufficient information for an accurate delineation of the target volume. Magnetic resonance imaging (MRI) can compensate for CT

in delineations of the target volume (3-5). Magnetic resonance imaging (MRI) provides superior image quality for soft-tissue delineation over computed tomography (CT) and is widely used for target and organ delineation in radiotherapy for treatment planning (6-8). Despite MR's superior soft-tissue contrast, it has not replaced CT for treatment planning due to the lack of electron-density information and geometric distortions caused by magnetic inhomogeneity, nonlinear gradients, susceptibility and chemical shifts. This research proposed a method to combine MRI with assigned CT HUs to solve the problem of the deficiency of electron-density information. This approach may play a role in exploring the feasibility of using MRI for radiation therapy planning in the future.

The purpose of this article was to divide CT values into different intervals, investigate the effect of CT value variation on dosimetric results and propose a method to combine MRI with assigned CT values.

## MATERIALS AND METHODS

To assign a mean CT value to the same organ, it is important that the dose changes in the CT range of this organ are not obvious. Therefore, we studied the effect of CT value on dose calculation. Subsequently, the CT values of different tissues were sampled to determine the relationship between CT number intervals and human tissues. The mean CT value was reassigned based on the original CT image, and a new synthetic CT image was obtained. To investigate the effect of CT value variation on dosimetric results, the original CT images and the new synthetic CT images were compared for fifteen patients in the treatment planning systems.

### Patient data collection

Thirty patients (15 men, 15 women; median age, 53 years; age range, 45–65 years) were selected. In this retrospective study, CT imaging data from three different regions were used: head and neck (n = 10), thorax (n = 10) and

pelvic cavity (n = 10). The patients in each subgroup were randomly selected. All of the participants and data were obtained from Department of Radiation Oncology, Zhongnan Hospital of Wuhan University from June 1<sup>st</sup>, 2016 to June 1<sup>st</sup>, 2017.

CT scanning was performed using a Siemens Somatom. Sensation 16 row spiral CT (Siemens, Erlangen, Germany), with voltage 120 kV, current 120 mA, slice thickness 5 mm and pitch 1.125 mm. The treatment planning system was Varian Eclipse version 10.0 (Varian Medical Systems, Palo Alto, CA)

The target and OAR volumes were defined in accordance with the International Commission on Radiation Units and Measurements reports 50 and 62. All target volumes were delineated slice by slice on the treatment planning computed tomography scan.

### Sampling of the CT values of different tissues

The interval method is one of the most common methods of CT value partition. If the CT value of human tissue is divided into several intervals, the mass density of human tissue is also divided into several intervals. Assuming that each interval is a medium, the chemical composition of the medium remains unchanged. In this study, the CT values of different tissues (organs) were sampled. According to the dose equivalence principle, the CT value interval and the mean CT values of body tissue were determined. The CT values were obtained with the function of "area profile". Random sampling of CT values was performed on representative organs, and the same organ in each patient was repeated 10 times. The average CT value, standard deviation and 95% confidence interval were obtained by the Eclipse treatment planning system.

### Effect of CT values on dose calculation

The treatment planning system translated the CT values into the corresponding electron density according to the built-in CT value density conversion curve. The tissue inhomogeneity correction in the radiotherapy treatment planning systems was based on the electron densities determined by CT scanning.

*Int. J. Radiat. Res., Vol. 17 No. 3, July 2019*

Then, the dose distribution of the radiotherapy plan was obtained. The same organization's CT values will exhibit some variation due to the machine, scanning conditions, processing algorithms and other factors. However, these changes have little effect on dose calculation<sup>(5,6,9)</sup>. As demonstrated in table 1, for a specific organ, the CT value changes over an interval, and the rationality of the interval partition should be verified by the results of the dose calculation.

**Comparison of dosimetric parameters between the original CT images and the new assigned CT images**

In this retrospective study, ninety cervical cancer patients were selected. Random assignment of patient numbers was performed based on a random number table. Patient numbers 1 to 15 (median age, 46 years; age range, 34–59 years) were included. The patients selected for this retrospective study had all been previously treated. All patients had complete clinical treatment plans with targets defined by experienced physicians. The patients' treatment plans were constructed by radiotherapy assistants based on the CT study. The CT studies had all been previously registered at the Department of Radiation Oncology, Zhongnan Hospital of Wuhan University from June 1<sup>st</sup>, 2016 to June 1<sup>st</sup>, 2017. All plans were designed via intensity-modulated radiation therapy (IMRT). Eclipse ver. 10.0 was used for all

delineations, registrations, and dose calculations. The assigned CT values were assigned to different structures to form a synthetic CT image (figure 1). CT values of targets and organs at risk (OAR) were assigned according to Table 1. Other organs were assigned a uniform CT value of 20 HU, which is an average value of multiple organs.

The original CT images and the new synthetic CT images were compared for fifteen patients in the treatment planning systems with the same parameter. We simply copied the original plan onto the synthetic CT image without changing any parameters (including the planned field number, angle, and output dose per field). According to the normal tissue tolerance dose scale of the Department of Radiation Oncology, Zhongnan Hospital of Wuhan University, the percent differences in the DVH parameters of targets and organs were calculated.

**Statistical analysis**

Statistical analysis was performed with SPSS Statistics 19.0 software (SPSS Inc., Chicago, IL, USA). Differences between the original CT image and organ-assigned synthetic CT and original CT image and homogeneous assigned synthetic CT were assessed using the independent sample nonparametric test according to each parameter. P-values <0.05 were considered statistically significant.

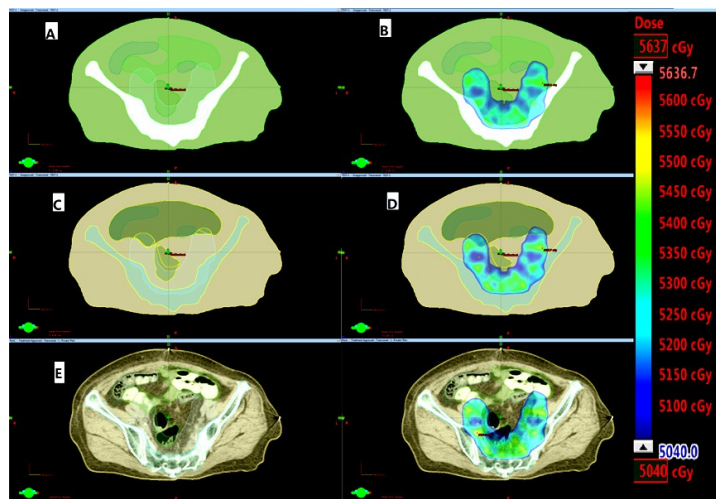


**Figure 1.** Homogeneous assigned synthetic CT (A); the dose distribution of the homogeneous assigned synthetic CT (B); organ assigned synthetic CT (C); the dose distribution of the organ assigned synthetic CT (D); original CT (E); and the dose distribution of the original CT (F).

## RESULTS

A virtual phantom in the Varian Eclipse treatment planning system was built with 6 MV. The prescribed CT values were between -1000 HU and 1000 HU, and the assignment interval was 50 HU. Figure 2A depicts the output dose curve.

Because the majority of the CT values of different tissues and organs range between -100 ~100 HU, except for lung and bone, a new statistic was calculated between -100 and 100

HU, and the assignment interval was 5 HU (figure 2B). The small figure depicts the output dose curve. The effect of CT value variation between -100 HU and 100 HU on dose calculation is within 3%, which can be ignored. The results demonstrate that the dose changed very slightly, which provided a reliable basis for CT synthesis. Subsequently, the dosimetric parameters were compared between the original CT images and the assigned new CT images after CT was synthesized, and the results are presented in table 1.

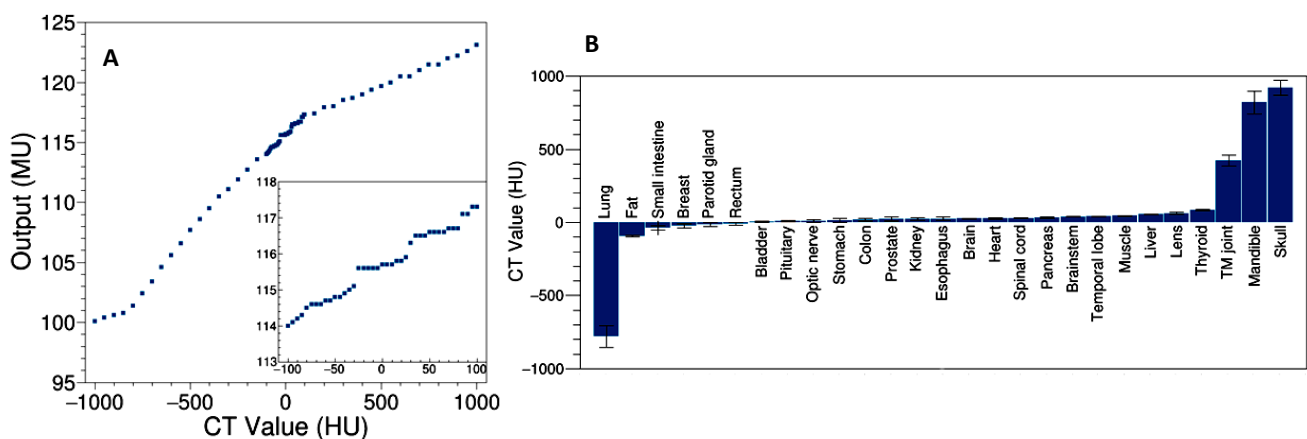


Figure 2. A; The output dose curve with 6 MV. B; The CT values of different tissues and organs.

Statistical analysis was performed with SPSS Statistics 19.0 software (SPSS Inc., Chicago, IL, USA).

Data fitting and drawing were based on Origin software (OriginLab, Northampton, Massachusetts, USA).

As shown in figure 2, the majority of the CT values of different tissues and organs ranged between -100 ~100 HU, with the exception of lung and bone.

Under the same treatment plan, there was no significant difference in the PTV and OAR dosimetry between the original CT image and the synthetic CT image ( $P > 0.05$ ). The deviation between the original CT image and the synthetic CT is presented in figure 3.

For the PTV, all deviations were less than 2%. The deviation between the original CT image and the homogeneous assigned synthetic CT image was larger than the deviation between the original CT image and the organ assigned

synthetic CT only for Dmax. For the PTV, organ assigned synthetic CT was closer to the original CT. For the left and right femoral head, the difference between the two assigned CT values was not obvious. Except for the left femoral head V50%, which was close to 3%, the other deviations were less than 2%. The reason for this difference may be that the femoral head contains cancellous and compact bone, and its CT value range fluctuates significantly. The femoral head cannot be assigned a uniform value and should be classified into compact and cancellous bone. The results of the small intestine were similar to those of PTV. With the exception of V60%, the deviations were less than 1.5%. For the bladder, the deviations between the original CT image and the homogeneous assigned synthetic CT were larger than those between the original CT image and the organ assigned synthetic CT with respect to Dmax, Dmean and V50%. However, all deviations were less than 1%, and the two

methods of synthetic CT were close to the original CT. The results for the rectum and bladder were similar. The reason for this variation may be because the organs are small and contain fluid. The organ assignment method was closer to the original CT value. The effect of CT value variation between -100 HU and 100 HU on the dose calculation was very small, as shown in figure 1, which includes the homogeneous assigned synthetic CT, organ assigned synthetic CT, original CT and the dose distribution of each CT image.

**Gamma pass rate**

The gamma pass rates are presented in table 2. Note: Group 1 includes the original CT and organ assigned synthetic CT. Group 2 includes the original CT and homogeneous assigned synthetic CT.

The results indicate that the gamma pass rates of the first group were higher than the second group. Only coronal planes (1 mm, 1%) exhibited statistically significant differences. There were no statistically significant differences between the other groups.

**Table 1.** The mean numbers and 95% confidence intervals of the major tissues and organs in three different regions

Organ / Tissue	95% confidence interval	Mean ± Standard deviation
<b>Head and neck</b>		
Parotid gland	-18.82~-10.97	-14.9±12.77
Pituitary	6.31 ~12.68	9.5±6.04
Optic nerve	5.16~14.57	9.87±8.21
Esophagus	19.24~31.07	25.15±11.84
Brain	24.78~28.91	26.85±3.64
Spinal cord	27.67~31.51	29.6±2.69
Brainstem	37.12~41.25	39.19±2.91
Temporal lobe	38.60~41.96	40.29±2.02
Lens	58.24~68.01	63.13±5.92
Thyroid	81.06~86.44	83.75±3.23
Temporomandibular joint	282.34~496.34	389.34±109.58
Mandible	779.82~919.32	849.57±64.08
Skull	874.34~964.37	919.36±50.23
<b>Thorax</b>		
Lung	-777.45~-749.24	-763.35±12.36
Fat	-96.05~-91.25	-93.66±6.44
Breast	-45.70~-4.89	-25.3±13.8
Stomach	10.16~20.89	15.53±14.11
Heart	25.16~32.46	28.82±4.4
Liver	54.03~56.07	55.06±3.59
<b>Pelvic cavity</b>		
Small intestine	-49.34~-26.73	-38.04±14.76
Rectum	-20.79~0.48	-10.15±8.19
Bladder	2.89~7.062	4.98±3.07
Colon	8.62~26.70	17.67±9.31
Prostate	9.04~36.28	22.67±12.59
Femoral head	365.47~519.57	449.35±68.26
The pelvis (cortex)	685.23~917.46	795.73±110.52
The pelvis (medulla)	67.63~149.98	110.23±30.87
Kidney	20.77~25.54	23.16±9.99
Pancreas	30.11~38.38	34.25±4.77
Muscle	44.35~47.84	46.1±2.76

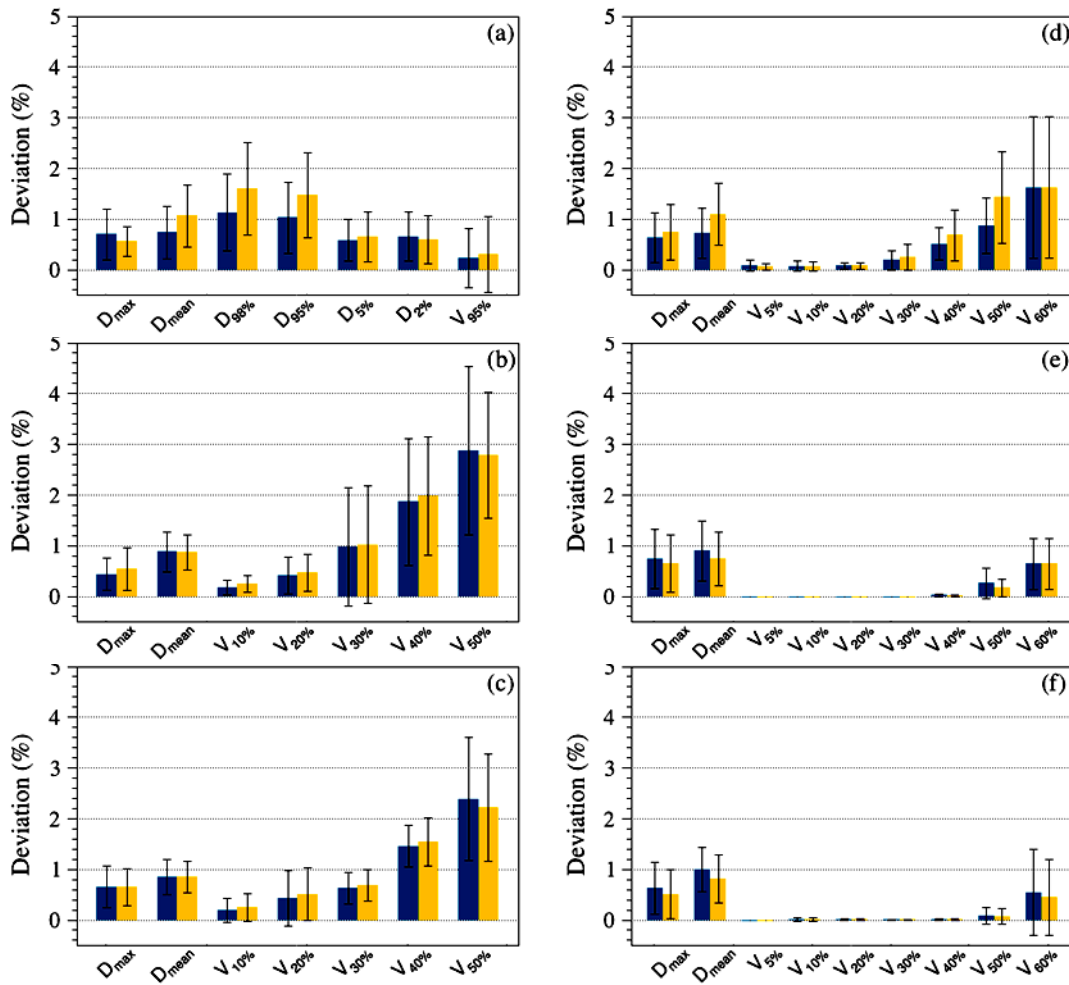


**Figure 3.** The blue bars reflect the deviation between the original CT image and the organ-assigned synthetic CT. The yellow bars reflect the deviation between the original CT image and homogeneous assigned synthetic CT. **(a):** PTV; **(b):** left femoral head; **(c):** right femoral head; **(d):** small intestine; **(e):** bladder; **(f):** rectum.

**table 2.** The gamma pass rates of different planes between two group assigned synthetic CT plans and original CT plan.

Result Groups	Gamma pass rate (1 mm, 1%)			Gamma pass rate (2 mm, 2%)		
	Cross plane	Coronal lane	Sagittal plane	Cross plane	Coronal plane	Sagittal plane
1	98.002	97.618	97.228	99.626	99.623	99.807
2	95.699	93.944	95.036	99.486	99.620	99.800
P Values	0.217	0.047	0.088	1.00	1.00	0.217

## DISCUSSION

In recent years, with the rapid development of radiotherapy technology, computer technology and medical imaging technology, treatment planning systems have been widely used for simulation and treatment dose calculation.

Computed tomography (CT) has been the ba-

sis for three-dimensional treatment planning systems (3D TPS) because the TPS can translate CT values into the corresponding electron density, according to the built-in CT value density conversion curve. Tissue inhomogeneity corrections in radiotherapy treatment planning systems are determined by CT scanning based on electron densities to obtain the dose distribution of the radiotherapy plan.

A phantom tissue or organ has different CT values and different relative electron densities in different reports. The CT value of the same tissue can also change under different scanning conditions<sup>(9-11)</sup>. Cozzi *et al.* have demonstrated that the variation in the voltage can shift the reconstructed Hounsfield numbers systematically by approximately 300 HU<sup>(15)</sup>. Hendee *et al.* have demonstrated that different CT scanners with different internal filtering algorithms can alter the CT value<sup>(9)</sup>.

The density of pelvic organs and tissues was relatively similar, and the deviation of the CT value had less effect on dose calculations. In the same interval, the mass density of the medium was linear with the CT value<sup>(12)</sup>. Walters *et al.* suggested that CT data should be binned into four major material groups: air, lung, soft tissue and bone<sup>(13)</sup>. Demarco *et al.* described CT data binned into five major material groups: lung, fat, water, muscle, and bone<sup>(14)</sup>. Alfidi *et al.* binned the CT data into six major material groups: air, lung, fat, water, muscle, and bone<sup>(15)</sup>. By contrast, Schneider *et al.* proposed binning CT data into twenty-four major material groups<sup>(16)</sup>. In the present study, although the organs were inhomogeneous, the variation in CT values fell within a certain range, which is the same as reported by Jonsson<sup>(5)</sup>, Lee<sup>(6)</sup>, and Hendee<sup>(9)</sup>. Therefore, many scholars can use the interval method to replace the CT value of real organs for research, as described by Walters<sup>(13)</sup>, Demarco<sup>(14)</sup>, Alfidi<sup>(15)</sup> and Schneider<sup>(16)</sup>.

In this paper, the mean CT values, sampled from different tissues, were reassigned on the original CT image, and a new synthetic CT image was obtained. To investigate the effect of CT value variation on dosimetric results, the original CT images and the new synthetic CT images were compared for fifteen patients in the IMRT treatment planning systems. Figures 3-8 and table 2 demonstrate that the deviation between the synthetic CT image and the original CT image were less than 2% in the PTV and OAR (bladder, rectum, small intestine, femoral head, etc.).

According to the normal tissue tolerance dose scale of the Department of Radiation Oncology, Zhongnan Hospital of Wuhan

University, we can see that the deviation is within the prescribed scope. The dose distribution is closer to the actual situation, and two DVHs have little difference. Therefore, the results satisfy the clinical requirements.

Some studies have explored the feasibility of MRI-based treatment planning, although the research methods of each scholar are different. Chen *et al.* studied the pair of MR and CT images that was preregistered using deformable image registration (DIR)<sup>(17-20)</sup>. Radiotherapy planning was performed on new synthetic CT images with electron density information<sup>(18)</sup>. Johansson *et al.* studied a Gaussian mixture regression model that was used to link the voxel values in CT images to the voxel values in images from three MRI sequences, and a new synthetic CT image was generated<sup>(19)</sup>. Acharya *et al.* reported the feasibility of online adaptive magnetic resonance image-guided radiation therapy (MR-IGRT)<sup>(20)</sup>.

In this paper, the problem of missing electron density information in the application of MRI in radiotherapy planning was preliminarily studied. There are some limitations to this research. For example, sampling methods need to be further optimized. Additionally, the sample size is small.

Through this research, we hope to propose a method to combine MRI with assigned CT values to solve the problem of the lack of electron-density information and hope that this study might play a role in exploring the feasibility of magnetic resonance imaging (MRI) for radiation therapy planning in the future.

**Conflicts of interest:** Declared none.

## REFERENCES

1. Buzug Thorsten M (2008) Applications in radiotherapy treatment planning. *Radiotherapy and Oncology*, **42(1)**: 1-15. Computed tomography: from photon statistics to modern cone-beam CT [M]. Springer Science & Business Media. DOI: 10.1007/978-3-540-39408-2
2. Khoo VS, Dearnaley DP, Finnigan DJ, Padhani A, Tanner SF, Leach MO, et al. (1997). Magnetic resonance imaging (MRI): considerations and applications in radiotherapy treatment planning. *Radiotherapy and Oncology*, **42(1)**: 1-

- 15.
3. Debois M, Oyen R, Maes F, Verswijvel G, Gatti G, Bosmans H, Vanuytsel L, et al. (1999) The contribution of magnetic resonance imaging to the three-dimensional treatment planning of localized prostate cancer. *International Journal of Radiation Oncology • Biology • Physics*, **45(4)**: 857-865.
4. Hricak, H. (1994). Mr imaging and mr spectroscopic imaging in the pre-treatment evaluation of prostate cancer. *Br J Radiol*, *78 Spec No 2(special\_issue\_2)*, S103.
5. Jonsson JH, Karlsson MG, Karlsson M, Nyholm T (2010) Treatment planning using MRI data: an analysis of the dose calculation accuracy for different treatment regions. *Radiation oncology*, **5(1)**: 62.
6. Lee YK, Bollet M, Charles-Edwards G, Flower MA, Leach MO, McNair H, Webb S, et al. (2003) Radiotherapy treatment planning of prostate cancer using magnetic resonance imaging alone. *Radiotherapy and oncology*, **66(2)**: 203-216.
7. Chen L, Price RA, Wang L, Li J, Qin L, McNeeley S, Pollack A, et al. (2004) MRI-based treatment planning for radiotherapy: dosimetric verification for prostate IMRT. *International Journal of Radiation Oncology • Biology • Physics*, **60(2)**: 636-647.
8. Lambert J, Greer PB, Menk F, Patterson J, Parker J, Dahl K, Kumar M, et al. (2011) MRI-guided prostate radiation therapy planning: Investigation of dosimetric accuracy of MRI-based dose planning. *Radiotherapy and Oncology*, **98(3)**: 330-334.
9. Khadivi KO. (2007). Computed tomography: fundamentals, system technology, image quality, applications, 2nd edition. *Clinical Imaging*, **31(3)**: 218.
10. Cozzi L, Fogliata A, Buffa F, Bieri S (1998) Dosimetric impact of computed tomography calibration on a commercial treatment planning system for external radiation therapy. *Radiotherapy and oncology*, **48(3)**: 335-338.
11. Sannazzari GL, Ragona R, Ruo Redda MG, Giglioli FR, Isolato G, Guarneri A, et al. (2002) CT–MRI image fusion for delineation of volumes in three-dimensional conformal radiation therapy in the treatment of localized prostate cancer. *The British journal of radiology*, **75(895)**: 603-607.
12. Wang L, Chui CS, Lovelock M (1998) A patient-specific Monte Carlo dose-calculation method for photon beams. *Medical physics*, **25(6)**: 867-878.
13. Walters B, Kawrakow I, Rogers DWO (2005) DOSXYZnrc user's manual. NRC Report PIRS, 794.
14. DeMarco JJ, Solberg TD, Smathers JB (1998) A CT-based Monte Carlo simulation tool for dosimetry planning and analysis. *Med Phys*, **25(1)**: 1-11. DOI: 10.1118/1.598167.
15. Alfydi RJ, Macintyre WJ, Meaney TF, Chernak ES, JAnicki P, Tarar R, Levin H, et al. (1975) Experimental studies to determine application of CAT scanning to the human body. *American Journal of Roentgenology*, **124(2)**: 199-207.
16. Schneider W, Bortfeld T, Schlegel W (2000) Correlation between CT values and tissue parameters needed for Monte Carlo simulations of clinical dose distributions. *Physics in Medicine & Biology*, **45(2)**: 459.
17. Stanescu T, Jans HS, Pervez N, Stavrev P, Fallone BG (2008) A study on the magnetic resonance imaging (MRI)-based radiation treatment planning of intracranial lesions. *Physics in Medicine & Biology*, **53(13)**: 3579.
18. Chen S, Quan H, Qin A, Yee S, Yan D (2016) MR image-based synthetic CT for IMRT prostate treatment planning and CBCT image-guided localization. *Journal of applied clinical medical physics*, **17(3)**: 236-245.
19. Johansson A, Karlsson M, & Nyholm T (2011) CT substitute derived from MRI sequences with ultrashort echo time. *Medical physics*, **38(5)**: 2708-2714.
20. Acharya S, Fischer-Valuck BW, Kashani R, Parikh P, Yang D, Zhao T, Rodriguez V, et al. (2016) Online magnetic resonance image guided adaptive radiation therapy: first clinical applications. *International Journal of Radiation Oncology • Biology • Physics*, **94(2)**: 394-403.